Neon seeding effects on two JET high performance baseline plasmas

S. Gabriellini[1], V.K. Zotta[1], L. Garzotti[2], C. Bourdelle[3], F.J. Casson[2], J. Citrin[4,5], D. Frigione[6], R. Gatto[1], E. Giovannozzi[7], C. Giroud[2], F. Koechl[2], P. Lomas[2], M. Marin[4], G. Pucella[7], F. Rimini[2], D. Van Eester[8] and JET Contributors*

[1] *Sapienza University of Rome, Rome, Italy*
[2] *CCFE, Culham Science Centre, Abingdon, UK*
[3] *CEA, IRFM, F-13108 Saint Paul Lez Durance, France*
[4] *DIFFER - Dutch Institute for Fundamental Energy Research, Eindhoven, the Netherlands*
[5] *Science and Technology of Nuclear Fusion Group, Eindhoven University of Technology, Eindhoven, Netherlands*
[6] *University of Tor Vergata, Rome, Italy*
[7] *ENEA C. R. Frascati, Frascati, Italy*
[8] *Laboratory for Plasma Physics, LPP-ERK/KMS, Bruxelles BE*
** See the author list of J Mailloux et al. 2022 Nucl. Fusion https://doi.org/10.1088/1741-4326/ac47b4*

1. Introduction Neon seeding on JET has been proved to be compatible with high performance plasmas and can lead to higher confinement with respect to the equivalent unseeded pulses [1]. In addition to this, neon is also needed for mitigating heat fluxes to the divertor.
In this paper we present the results of the predictive modelling performed on two JET baseline ELMy H-modes, a Ne-seeded pulse (JPN 96994) and an equivalent unseeded one (JPN 96730), carried out with the JINTRAC suite of codes and the QuaLiKiz transport model. The baseline scenario is one of the scenarios envisaged for achieving high fusion power with a steady performance, characterised by high plasma current and moderate normalised beta [2]. The pulses share the same main plasma parameters, however, the Ne-seeded shot exhibits a slightly higher confinement and performance with respect to the unseeded one.
In section 2 we describe the shots and the modelling settings, in section 3 we compare the QuaLiKiz turbulence spectra and discuss the neon effects on transport and in section 4 we draw some conclusions.

2. Modelling the discharges The shots analysed in this work are two baseline ELMy H-modes, with $I_p = 3.0$ MA, $B_T = 2.8$ T and $\beta_N = 2.2$. The time interval chosen for the analysis is between 10 and 12 seconds and the experimental parameters listed in this paper are averaged over the modelled time interval. The neon seeded shot (JPN 96994) has an additional heating power of 31 MW, 28 MW from neutral beam injection (NBI) and 3.3 MW from ion cyclotron resonance heating (ICRH) in H minority scheme. The unseeded shot (JPN 96730) has a slightly higher power of 33 MW, 29 MW from NBI and 4.1 MW from ICRH in H minority scheme. One of the main differences between the pulses is the lower electron density pedestal and the higher core ion temperature of JPN 96994 with respect to JPN 96730. The higher core ion temperature is probably due to the higher ion temperature pedestal, which propagates into the core because of the stiffness of the profiles. Both of these differences are contributing to the performance and to the confinement of the Ne-seeded discharge, which are reflected respectively in the higher neutron rate (~ +11.4%) and in the higher energy confinement time τ_E (~ +11.5%). The goal of the modelling is therefore to understand whether the higher confinement of JPN 96994 has to be ascribed solely to the pedestal improvement with neon or if a different core transport mechanism is at play.
The simulations are performed in a fully predictive way in the JINTRAC [3] suite of codes, using the JETTO [3] transport solver and the QuaLiKiz [5, 6] first-principle transport model, which is a quasilinear gyrokinetic code used to compute the turbulent transport from the magnetic axis up to the pedestal top. In our simulations we are modelling the evolution of the plasma current density, ion density, electron and ion temperature and plasma rotation, as well as the evolution of the impurities density. The impurity transport is calculated by SANCO [7] which takes into account an impurity mix of Be, Ne, Ni and W, whose relative concentrations are prescribed according to an estimate described in [8]. The boundary conditions are imposed at the separatrix which is considered to be the position in which $T_e = T_i = 100$ eV, while the initial conditions for the electron density and temperature profiles

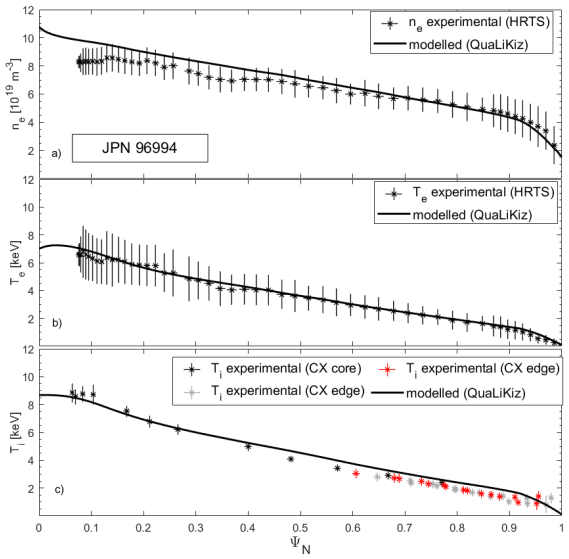

Figure 1: comparison between the experimental and the modelled electron density (a), electron temperature (b) and ion temperature (c) profiles of JET shot 96994 (Ne-seeded).

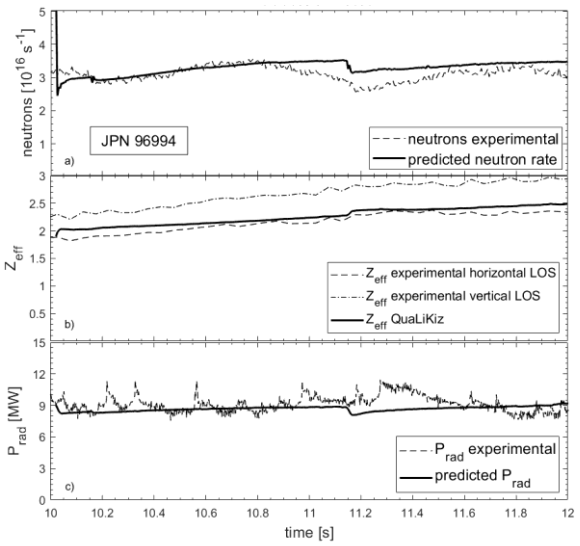

Figure 2: comparison between experimental and modelled neutron rate (a), Z_{eff} (b) and bulk radiative power (c) of JET shot 96994 (Ne-seeded).

are taken from the measurements of the JET high resolution Thomson scattering (HRTS) system [9] and for the ion temperature profiles from beam charge exchange (CX) spectroscopy [10].

The heat transport in the edge transport barrier (ETB) is adjusted in order to match the experimental height of the temperature pedestal. The width of the pedestal is imposed to match the experimental value. Once the heat transport in the ETB has been fixed, we assumed $\chi/D = 4$ in the pedestal and tuned the gas puff particle source to match the density at the top of the ETB. This methodology has been presented and validated in [11].

The equilibrium is computed self-consistently with the evolution of the kinetic profiles and the current density profile using the ESCO equilibrium solver [12]. The heat sources are computed by the PENCIL [13] and PION [14] codes for the NBI and the ICRH respectively, where the synergy is taken into account self-consistently in JINTRAC [15].

The profiles and time traces of the simulations are compared against the experimental values in figures 1 and 2 for JET shot 96994 and in figures 3 and 4 for JET shot 96730. From this comparison it can be seen that there is a general good agreement between the experiment and the simulations, especially in the pedestal values, meaning not only that QuaLiKiz is able to capture the transport in the core, but also that the empirical modelling of the pedestal is valid.

3. Neon effects on transport

After well reproducing the discharges with the QuaLiKiz transport model, it is possible to investigate the difference in transport between the two shots. What emerges from the modelling is that QuaLiKiz shows a reduction in the ion and electron thermal diffusivities of the Ne-seeded pulse with respect to the equivalent unseeded one, which can be seen in figure 6. This effect can also be seen in the reduction of the heat fluxes of JPN 96994, which is stronger for the ions than for electrons. In order to understand the cause of the transport reduction, QuaLiKiz turbulence spectra are compared in figure 5. It is important to underline that the QuaLiKiz dispersion relation accounts for trapped and passing ions and electrons, i.e. it covers the ITG-TEM and ETG ranges. In the figure, $k_\theta\rho_s$ is the product of the poloidal wavenumber k_θ and the main ion gyroradius ρ_s, while γ/k_θ^2 is the growth rate of the turbulence normalised to the square of the poloidal wavenumber; the growth rates are averaged between [11.37 - 11.87 s], in order to avoid the impact of sawteeth in the shots. It can be seen that, according to the QuaLiKiz microstability analysis, the seeding of neon causes a reduction in the growth rates of both ITG (low $k_\theta\rho_s$) and ETG (high $k_\theta\rho_s$) modes. The turbulence stabilization can be caused by a series of non-linear effects which can be difficult to disentangle from each other. It has been argued in other papers (see [16]) that the impurities play a role in the stabilization of the ETG modes, while **E** *x* **B** shear stabilizes the lower-k part of the spectrum, i.e. ITG modes. The same type of study presented here and performed with the GENE code for JPN 96994 shows similar results and can be found in [17]. In addition to this, because

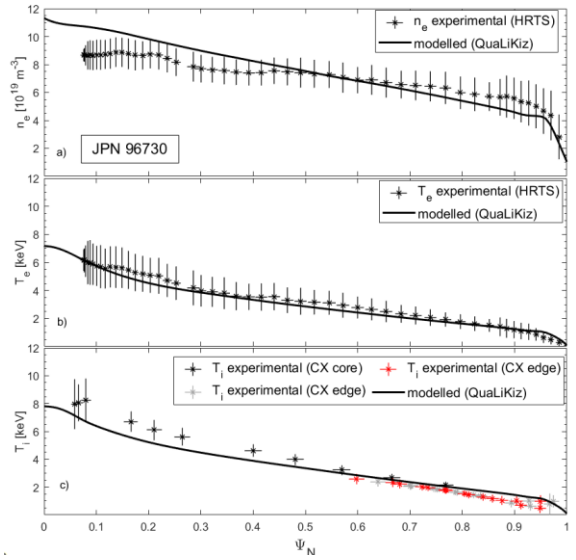

Figure 3: comparison between the experimental and the modelled electron density (a), electron temperature (b) and ion temperature (c) profiles of JET shot 96730 (unseeded).

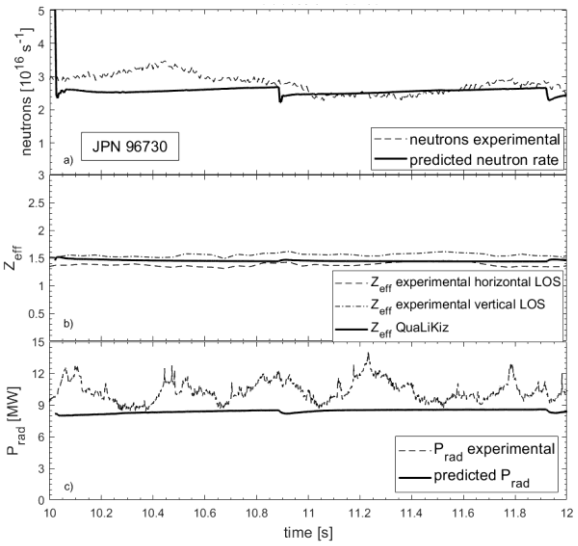

Figure 4: comparison between experimental and modelled neutron rate (a), Z_{eff} (b) and bulk radiative power (c) of JET shot 96730 (unseeded).

of the higher T_i/T_e ratio of JPN 96994 with respect to JPN 96730, a stronger positive feedback between high T_i/T_e ratio and ITG stabilization could be present in the Ne-seeded shot [18]. Overall, integrated modelling performed on different Ne-seeded JET pulses, described in [1, 19], shows similar results to the ones presented in this work, identifying in the reduced core transport (via ETG and ITG turbulence stabilization) and in the increased pedestal T_i and T_e the causes for the improved performance with neon. However, it is important to underline that the shot analysed here has a lower neon seeding ($\Gamma_{Ne} = 8 \cdot 10^{21}$ el/s), lower recycling, lower gas puff ($\Gamma_D = 1.2 \cdot 10^{22}$), lower edge collisionality and an higher performance with respect to the ones described in [1, 19], which are shots that are pushed towards detachment.

Further modelling was carried out in order to disentangle the two main effects of neon on transport, which are a direct effect on the turbulence stabilization and an accompanying effect on the pedestal parameters, both causing an improvement in performance and confinement. Two simulations, based on the reference modelling of JPN 96730 shown in figures 3 and 4, were performed: a first one in which we imposed the same pedestal settings used to model JPN 96994 and a second one in which we imposed the same neon seeding rate as the one used for JPN 96994. In figure 7 we can see the results in terms of the average neutron rates of the simulations, normalised to the simulated performance of JPN 96994. We can see that the neutron rate of the unseeded shot improves on average of ~ 5 % when neon is injected into the plasma and of ~ 17 % when we are imposing the pedestal of the Ne-seeded shot. Assuming a linear combination of the two effects, we can see that we recover the performance of JPN 96994. However, a plasma is an highly non-linear system, so it is probable that the two effects are indeed interacting with each other.

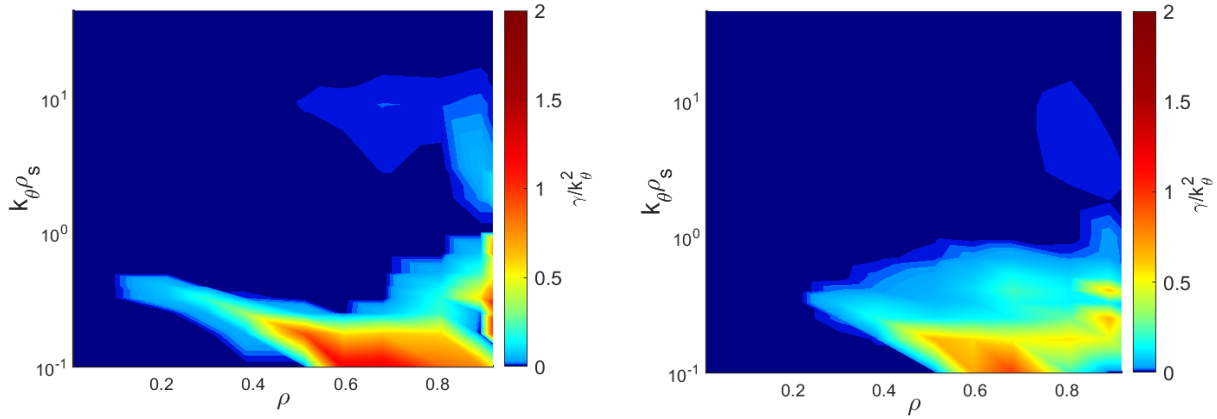

Figure 5: QuaLiKiz turbulence spectra for JET shot 96370 (left box) and JET shot 96994 (right box). On the x-axis we have the JETTO normalised coordinate ρ, on the y-axis there is the product of the poloidal wavenumber k_θ and the main ion gyroradius ρ_s, while the colormap represents the growth rate γ of the turbulence normalised to the square of the poloidal wavenumber k_θ^2. The growth rates are averaged between 11.37 and 11.87 seconds, in order to avoid the impact of sawteeth.

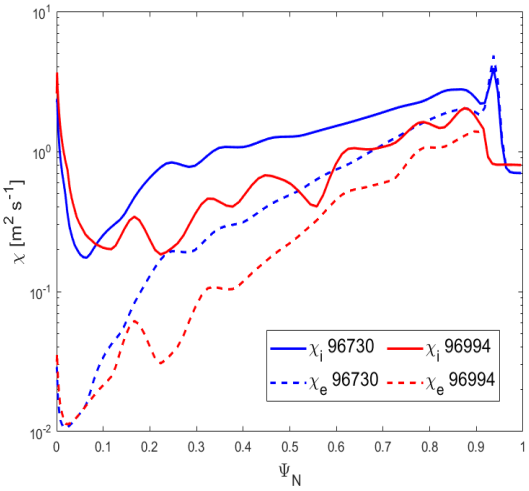

Figure 6: electron (dashed line) and ion (solid line) thermal diffusivities for JPN 96994 (red) and JPN 96730 (blue), averaged between [11.37 - 11.87s] and plotted in logarithmic scale.

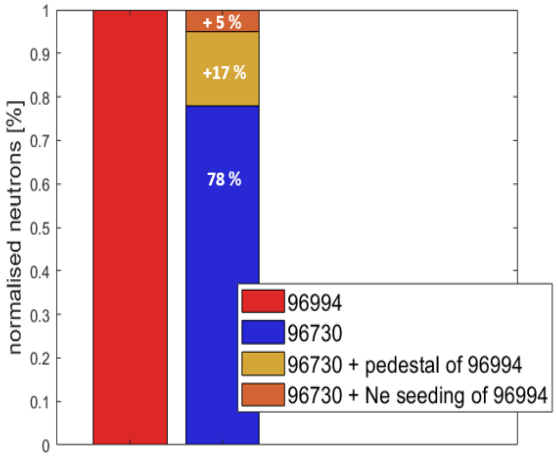

Figure 7: averaged neutron rates normalised to the performance of the reference modelling of JPN 96994. Imposing the pedestal characteristics of JPN 96994 on JPN 96730 allows to gain ~ 17% on performance, while imposing the Ne seeding rate allows to gain ~5%.

4. Conclusions

In this work we have presented the JETTO-QuaLiKiz-SANCO fully predictive modelling of two JET high performance baseline plasmas, a Ne-seeded pulse (JPN 96994) and an equivalent unseeded one (JPN 96730). The simulations are in good agreement with the experimental measurements for both of the analysed shots, therefore allowing QuaLiKiz to capture the differences in transport between the pulses.

The transport model shows a reduction in the core ion and electron thermal diffusivities of the neon seeded shot with respect to the unseeded ones. The comparison of QuaLiKiz turbulence spectra suggests that Ne injection reduces the growth rates of both ETG and ITG modes, leading to a decrease of the electron and ion heat fluxes with respect to the unseeded pulse.

Further modelling of the discharges suggests that the experimentally observed confinement improvement obtained with neon seeding is caused by a combination of improved pedestal parameters and turbulence stabilization by Ne injection.

Acknowledgements This work has been carried out within the framework of the EUROfusion Consortium, funded by the European Union via the Euratom Research and Training Programme (Grant Agreement No 101052200 — EUROfusion). Views and opinions expressed are however those of the author(s) only and do not necessarily reflect those of the European Union or the European Commission. Neither the European Union nor the European Commission can be held responsible for them.

References

[1] Giroud C. et al, "*High performance Ne-seeded baseline scenario in JET-ILW in support of ITER*" (2022) at 48th EPS Conference on Plasma Physics (I4.108)
[2] L. Garzotti et al 2019 Nucl. Fusion **59** 076037
[3] Romanelli M. *et al* 2014 *Plasma Fusion Res.* **9** 3403023
[4] Cenacchi G and Taroni A 1988 JETTO: a free boundary plasma transport code ENEA Report RT/TIB/88/5
[5] Bourdelle C., Citrin J., Baiocchi B., Casati A., Cottier P., Garbet X. and Imbeaux F. 2016 *Plasma Phys. Control. Fusion* **58** 014036
[6] Citrin J. *et al* 2017 *Plasma Phys. Control. Fusion* **59** 124005
[7] Lauro Taroni L. 1994 *Proc. 21st EPS Conf. Controlled Fusion and Plasma Physics ECA* (Montpellier, France, 27 Jun–1 Jul 1994) vol 18B part I p 102
[8] Sertoli M., Carvalho P.J., Giroud C. and Menmuir S. 2019 *J. Plasma Phys.* **85** 905850504
[9] Pasqualotto R., Nielsen P., Gowers C., Beurskens M., Kempenaars M., Carlstrom T. and Johnson D. 2004 *Rev. Sci. Intrum.* **75** 3891
[10] Hawkes N.C., Delabie E., Menmuir S., Giroud C., Meigs A.G., Conway N.J., Biewer T.M. and Hillis D.L. 2018 *Rev. Sci. Instrum.* **89** 10D113
[11] V.K. Zotta *et al* 2022 *Nucl. Fusion* **62** 076024
[12] Cenacchi G. and Rulli M. 1988 Upgrading of an equilibrium transport code for a multispecies free-boundary plasma *ENEA Report RTI/TIB(88)5*
[13] Challis C.D., Cordey J.G., Hamn´en H., Stubberfield P.M., Christiansen J.P., Lazzaro E., Muir D.G., Stork D. and Thompson E. 1989 *Nucl. Fusion* **29** 563
[14] Eriksson L.-G., Hellsten T. andWill´en U. 1993 *Nucl. Fusion* **33** 1037
[15] Gallart D. *et al* 2018 *Nucl. Fusion* **58** 106037
[16] G. M. Staebler et al, 1999, Phys. Rev. Lett. **82**, 1692
[17] J. Garcia et al Phys. Plasmas 29, 032505 (2022)
[18] Hyun-Tae Kim *et al* 2018 *Nucl. Fusion* **58** 03
[19] Marin M. et al *"Integrated modelling of Neon impact on JET H mode core plasmas"* submitted to Nucl. Fusion